JOURNAL OF MATERIALS SCIENCE 20 (1985) 4084–4090

Surface damage of single-crystal silicon abraded in ethanol and deionized water

D. S. LIM, S. DANYLUK
Department of Civil Engineering, Mechanics and Metallurgy, University of Illinois at Chicago, Chicago, Illinois 60680, USA

Semiconductor grade, single-crystal silicon wafers of (1 0 0) p-type were abraded by a single-point, slow speed (2.3 cm sec^{-1}) 90° pyramid diamond in ethanol and deionized water. The scratching was carried out in each of the fluids with a load of 0.5 N on the sliding diamond. The scratching produces a groove, the depth of which depends on the number of traverses of the diamond. A measure of the cross-sectional area of the groove was used to determine the abrasion rate in ethanol, which was about 1.3 times that in deionized water. Some of the samples scratched in deionized water were annealed at 1000° C for 1 h and these samples, along with those unannealed and scratched in both fluids, were fractured perpendicular to the scratch in a three-point bend apparatus. The fracture strengths and the mirror distances obtained by scanning electron microscope (SEM) observation were used to deduce tensile residual stresses of 15.6 and 99.0 MN m^{-2} beneath the grooves formed in deionized water and ethanol, respectively. The SEM investigation also showed that (a) the groove surfaces contained microcracks wedged with wear debris, and (b) dislocations were generated and propagated away from the groove surfaces as a result of annealing. The relatively higher tensile residual stress produced in the presence of ethanol is consistent with the higher wear rate in this fluid.

1. Introduction

There has been renewed interest recently in the mechanical properties of semiconductors. Aside from purely academic interest, the mechanical strength [1, 2], fracture toughness [3] and plastic deformation [4, 5] are being studied because these properties can have an influence on the yield of silicon used for large-scale integrated circuits and solar cells. Abrasive cutting and polishing [6–8], processing steps used to produce desired shapes and surface smoothness, are of particular interest since these are the first process steps in fabricating devices. Abrasive wear is a complex process involving the contact of the abrading particle and the semiconductor surface with the concomitant fracture, and plastic deformation of one or both of the contacting surfaces.

Single-crystal silicon boules are cut into wafers by abrasive wear with diamond or silicon carbide impregnated wires or circular blades. After cutting, the wafers are polished in slurries containing abrasives such as Al_2O_3. Both processes result in microcracks and a permanently deformed (plastic) region on both surfaces of the wafer. This damage zone must be removed or minimized since the microcracks can be the cause of unexpected spontaneous brittle fracture [9] and the electrical properties can be adversely affected by microtwins and dislocations [7]. Abrasive wear is also used in the scribbing and dicing of the processed silicon wafers prior to thermocompression or diffusion bonding of the finished chips.

It is not always possible, however, to remove the damaged region from the wafer surfaces

0022–2461/85 $03.00 + .12 © *1985 Chapman and Hall Ltd.*

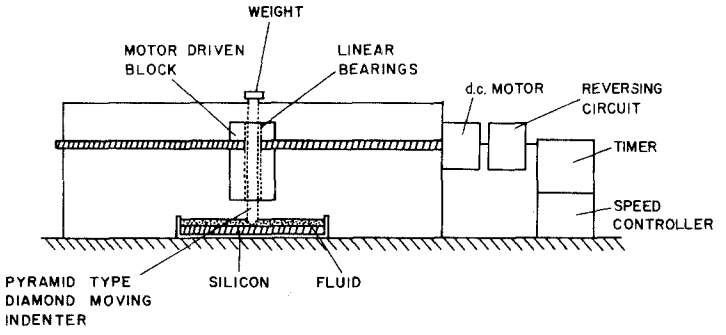

Figure 1 Schematic diagram of experimental apparatus.

since, once initiated, the cracks propagate on cleavage planes at relatively low stresses and the crack lengths can extend significantly beyond the immediate contact area of the diamond and the silicon. In addition, if the silicon surface region is plastically deformed then the dislocations and microtwins can extend to significant distances below the surface. The damaged region, therefore, will be composed of microcracks and a plastically deformed region and be the source of residual stresses that participate in the wear process. Although it is convenient to discuss the microcracking and plastic zone generation as separate processes during wear, there is an intimate connection between the two. As wear proceeds, the silicon deforms by the lowest energy process. If the silicon can relieve the imposed stresses by plastic deformation then the cracking propensity will be low and vice versa.

In this paper we summarize results of single-point scratching of (1 0 0) p-type single-crystal silicon wafers in ethanol and deionized water by the slow-speed sliding of a single-crystal 90° pyramid diamond, dead-weighted with 0.5 N. Ethanol and deionized water were chosen since these fluids have been shown to influence the microhardness of silicon [10] and it was expected that the surface deformation caused by scratching would also be affected. The wear was determined by measuring the cross-sectional area of the linear groove formed by scratching.

Randomly selected specimens that had been scratched in deionized water were annealed and the fracture strengths of these as well as the unannealed specimens scratched in each fluid were measured after three-point bending. The bending strength was correlated with fracture mirror measurements [11–13]. These measurements have been used to deduce the residual stresses in the vicinity of scratch grooves.

2. Experimental procedure

The experiments were carried out in the following way. Single-crystal silicon wafers of (1 0 0) p-type 0.5 mm thick, that had been lapped and polished according to semiconductor industry standards, were cut into 77.2 mm × 19.3 mm rectangular plates. These plates were dipped in a 10 vol % hydrofluoric acid bath for 30 sec, rinsed in deionized water and dried. The specimens were then immersed in either ethanol or deionized water and scratching was carried out within seven minutes. Fig. 1 shows a schematic diagram of the experimental arrangement. A 90° pyramid diamond is mounted in linear bearings to minimize frictional forces when a dead-weight load is applied. The diamond is also fixed to a worm gear that is driven by a d.c. motor. The silicon plate is fixed to a pedestal by spring tabs so that the diamond can traverse a straight-line path on the surface. Ethanol or deionized water is placed on the surface during scratching. The entire apparatus is in an enclosure that ensures only minor variations in temperature and humidity. The silicon plate geometry is chosen so that the long axis is ⟨1 1 0⟩ and the diamond generates a linear scratch along this direction. The velocity of the diamond was chosen to be 22.8 mm sec^{-1} and the length of the traverse was typically 50 mm. The depth of the groove was controlled by specifying the number of traverses made by the diamond or, equivalently, the time during which scratching was conducted. Randomly selected samples scratched in deionized water were annealed at 1000° C for 1 h in a purified argon environment.

Each of the samples was fractured in an Instron universal testing machine in a three-point bend fixture (according to ASTM D790) at room temperature. The cross-head speed was 0.01 in. min^{-1} (0.25 mm min^{-1}). Fig. 2 shows a schematic diagram of the silicon geometry and

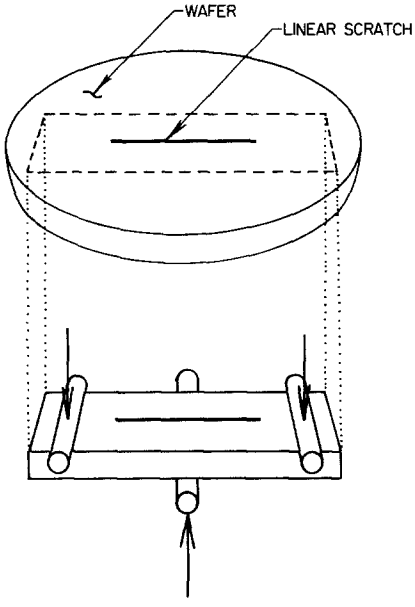

Figure 2 Schematic diagram of the three-point bend test for determination of fracture strength.

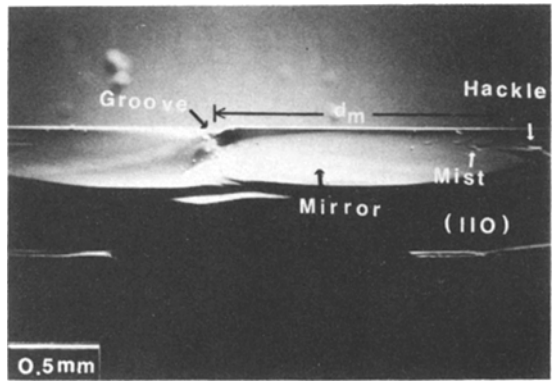

Figure 3 SEM micrograph of the (1 1 0) cleavage fracture surface. The linear multi-scratch groove produced by a 0.5 N dead-loaded pyramid diamond is shown in the cross-section. The bend test is conducted in air. The inset shown in the figure designates the locations of the groove, mirror and hackle region.

the three-point bend fixture. The fracture occurs perpendicular to the scratch.

The fracture surfaces were examined in the scanning electron microscope (SEM). Measurements of the groove area are used to determine the wear as a function of the number of scratches in the fluid. The measured fracture stress and the mirror distance determined in the SEM are used to obtain the residual stresses associated with the grooves formed in the fluids. Fig. 3 shows a typical cross-sectional (1 1 0) cleavage surface observed in the SEM. This figure shows the cross-sectional area of the groove and the morphology of the hackle region. The size of the mirror region is indicated by the mirror distance d_m which is measured for each sample. When the distances from the fracture origin are non-symmetric, the larger mirror distance is chosen as suggested by Freiman *et al.* [14].

3. Results and discussion

Fig. 4 shows SEM micrographs of the top view of the deionized water and ethanol grooves after a single scratch and ten scratches; all other environmental conditions were kept constant. As can be seen from these micrographs, the groove width after ten scratches is larger for the ethanol groove as compared with the deionized water groove. In addition, the single-scratch grooves have different crack morphologies from the multi-scratch grooves. The ethanol groove appears to contain flattened protrusions, and the cracks running perpendicular to the groove direction are longer as compared with the deionized water groove.

The groove area was measured as a function of the number of scratches and these data are shown in Fig. 5. As can be seen, the groove area increases with the number of scratches. The rate at which the groove area increases in size is larger for the ethanol groove as compared with the deionized water groove. The ratio of the two rates is 1.3:1. This difference in the wear rates for the two fluids was unexpected.

The bending strength plotted against the square root of the groove area, measured perpendicular to the scratch for the different environments, is shown in Fig. 6. The strength is high for small groove areas and decreases to a constant, relatively uniform value as the groove area increases. Since the groove area is small relative to the cross-sectional area of the sample and the groove is perpendicular to the applied bending moment, it does not significantly influence the fracture strength. However, the cracks, which are perpendicular to a scratch [15] and the accompanying residual stresses, affect the fracture strength. Therefore, the fracture strength is insensitive to groove area for each fluid. The damage is the predominant influence on fracture strength and more or less uniform for a particular fluid after many scratches. As shown in Fig. 6, silicon scratched in ethanol

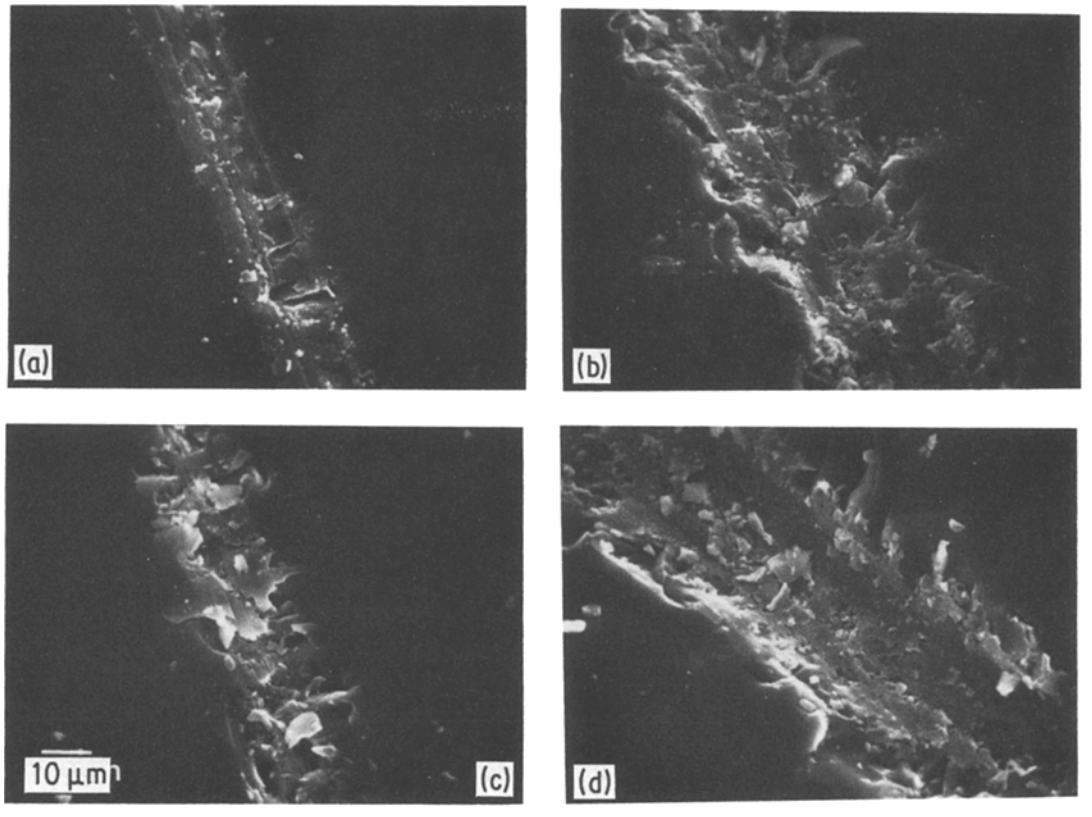

Figure 4 Scanning electron micrographs of a single scratch and ten scratches formed in deionized water and ethanol. Deionized water (a) single scratch, (b) ten scratches. Ethanol (c) single scratch, (d) ten scratches.

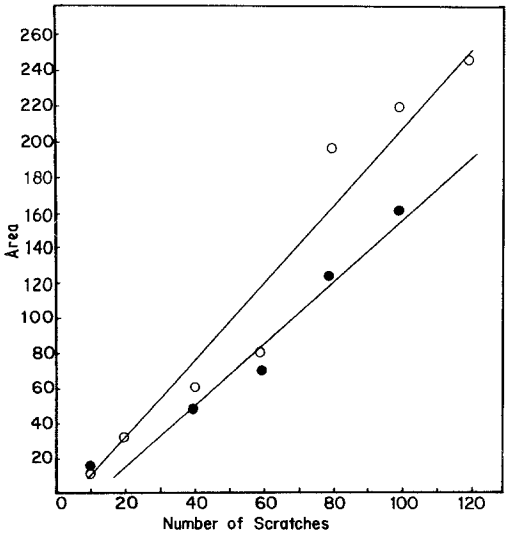

Figure 5 Groove area plotted against number of scratches. The groove area determined by SEM is larger for ethanol (○) than for deionized water (●).

shows approximately at 15% degradation of fracture strength compared to that scratched in deionized water. The difference in fracture strength between fluids is the result of microcracks around the groove and residual stresses caused by dislocations, as well as the wedging action of debris in the cracks.

Figs. 7 and 8 show SEM micrographs of cracks in the vicinity of grooves; these illustrate the wedging of microcracks by debris and evidence of plasticity in the vicinity of the grooves. Fig. 7 shows a micrograph of a groove fractured along the groove length. Microcracks extend into the silicon at an inclined angle to the sliding direction. The higher-magnification inset shows debris wedged in the crack. The debris prevents crack closure and, on multiple subsequent passes by the diamond, tensile wedge-opening stresses are generated that allow the cracks to propagate. Fig. 8 shows SEM

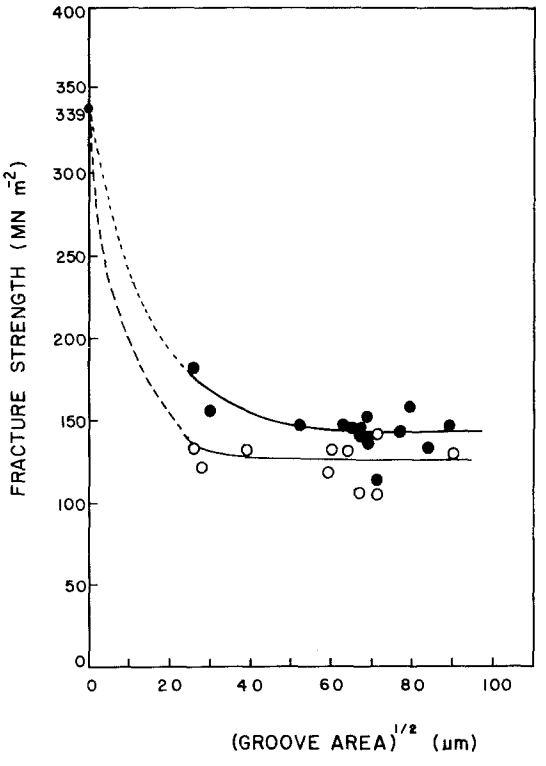

Figure 6 Bending strength plotted against square root of groove area for silicon fractured in air. A linear groove was formed on the (1 0 0) surface in the presence of (○) ethanol and (●) deionized water. The strength is independent of groove area. The unscratched strength is 339 MN m^{-2}.

micrographs of a typical groove annealed at 1000° C for 1 h. The higher-magnification inset shows dislocation etch pits revealed in a 10 glacial acetic acid : 1 HF : 3 HNO_3 solution [16] for 1.25 h. This figure indicates that dislocations are generated and propagated during annealing, with the propagation taking place in response to residual stresses in the vicinity of the groove.

The residual stresses may be deduced from a measurement of the fracture mirror distance of the annealed and unannealed samples. Fig. 9 show these results. Considering the data for the annealed samples in Fig. 9, it can be seen that the data are grouped about a mean fracture strength of 206.8 MPa and a mean mirror distance of 0.45 mm. If it is assumed that the annealing results in a diminution of the residual stress to zero, then the straight line drawn through the mean and the origin of this graph should have a slope which is the mirror constant, A.

The fracture strength and mirror distance for the annealed samples are related by

$$\sigma d_m^{1/2} = A \qquad (1)$$

where σ is the fracture stress, d_m is the distance from the groove to the onset of the hackle and A is the mirror constant. This relationship is

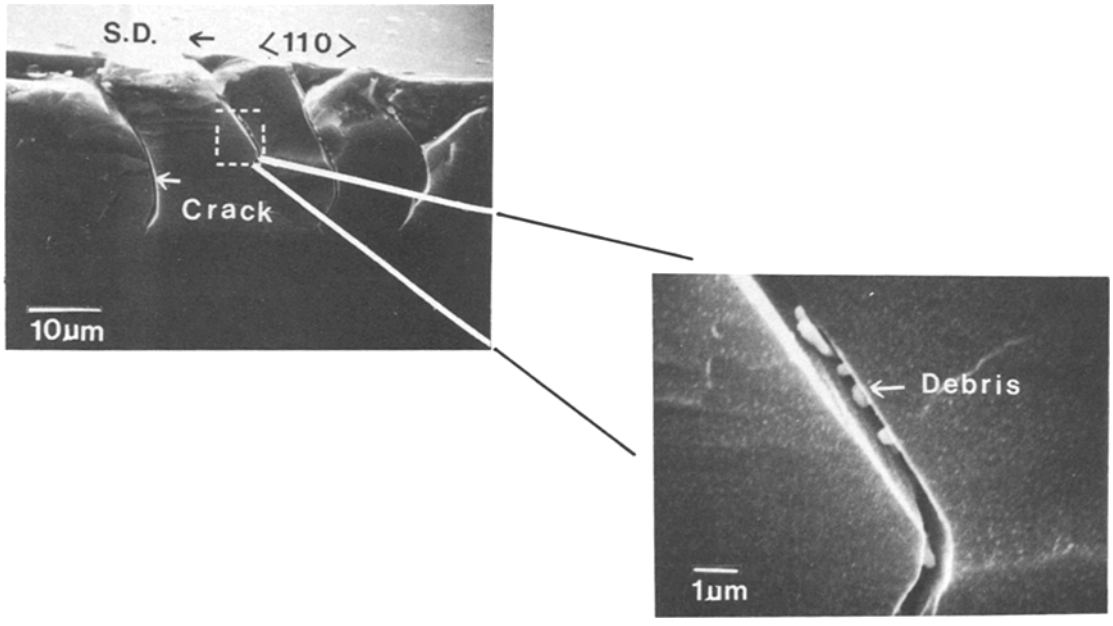

Figure 7 SEM micrograph of the groove fractured along the groove length; the scratch was formed in ethanol by 10 passes of the diamond. This groove was etched as described in the text. The cracks have debris wedged between the separated surfaces.

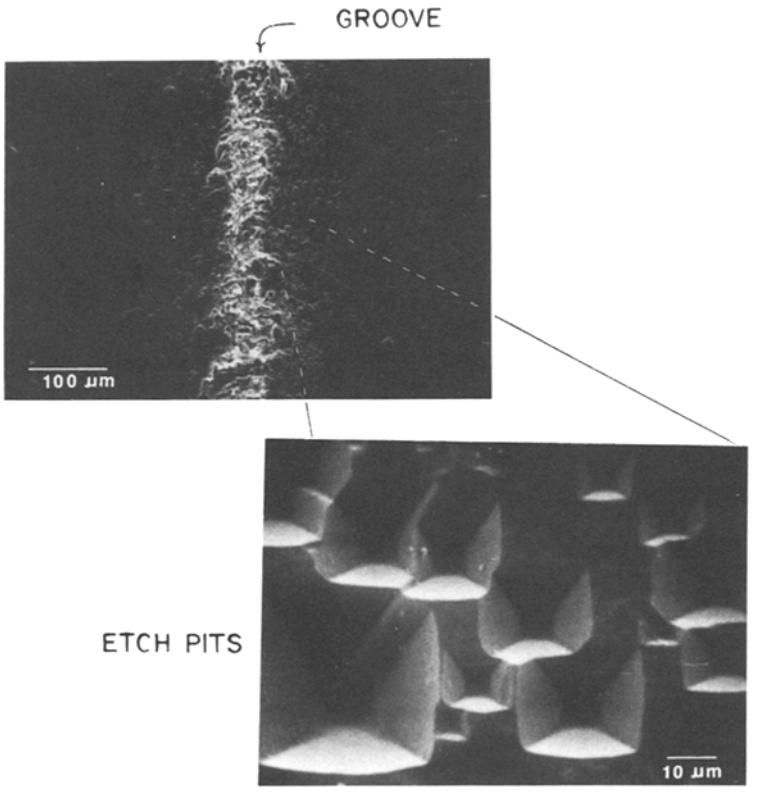

Figure 8 SEM micrographs of p-type silicon abraded in ethanol, annealed in argon at 1000° C for 1 h and etched for 10 glacial acetic acid : 1:HF : 3 HNO_3 solution [15] for 1.25 h.

modified to be

$$(\sigma_a + \sigma_R)\, d_{m_a}^{1/2} = A \qquad (2)$$

when a residual stress σ_R is present, as is the case for the unannealed samples. σ_a and d_{m_a} are the mean of the applied stress and the mirror distance of the unannealed specimens. This equation can be rearranged to give

$$\sigma_a d_{m_a}^{1/2} + \sigma_R d_{m_a}^{1/2} = A \qquad (3)$$

so that

$$\sigma_R = (A - A_{eff})\, d_{m_a}^{-1/2} \qquad (4)$$

A is obtained from the slope of annealed deionized H_2O scratched samples. A_{eff} is the apparent slope of the unannealed samples in Fig. 9. Using the above equations, the residual stresses created during the scratching in ethanol and deionized H_2O are calculated to be 15.6 and 99.0 MN m^{-2}, respectively. This result shows that tensile residual stresses, perpendicular to the scratching direction, are present as a result of scratching in both fluids. Since the residual stresses are higher for the ethanol grooves, the wear rate is expected to be increased since this residual stress will add to the applied stress in order to propagate microcracks and a plastic zone.

4. Conclusions

(a) The groove area and damage zone in the single-crystal silicon resulting from single-point multiple scratching are dependent on the fluids covering the silicon surface during scratching.

(b) The damage zone beneath the groove contains microcracks and a permanently deformed region which results in tensile stresses.

(c) The fracture strength of abraded silicon when fractured perpendicular to the scratching groove is not sensitive to the groove area but to the damage zone.

(d) Tensile residual stresses created during the scratching in ethanol and deionized water have been estimated to be 15.6 and 99.0 MN m^{-2} respectively. This result is consistent with the observation that the wear in ethanol is higher than in deionized water.

Acknowledgements

This research was supported by the Jet Propulsion Laboratory (JPL), Flat-Plate Solar Array

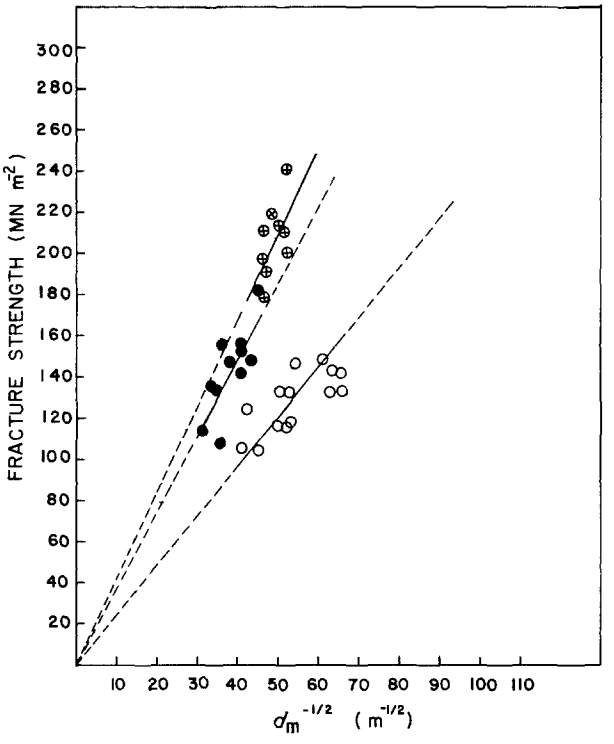

Figure 9 Applied stress plotted against $d_m^{1/2}$ for (⊕) annealed (1 h) and (●) unannealed silicon after scratching in deionized water, and (○) unannealed silicon after scratching in ethanol.

Project No. 956053. We are grateful for the support and encouragement of Drs K. M. Koliwad, M. Leipold, A. Morrison and C. P. Chen of JPL. The silicon wafers were provided by Mr J. Farber and Dr M. Kozak of Monsanto.

References

1. K. SUMINO, Proceedings of the 4th International Symposium on Silicon Materials and Technology, Semiconductor Silicon, Minneapolis, 1981 (Pennington, New Jersey, 1981), p. 208.
2. B. R. LAWN, D. B. MARSHALL and P. CHANTIKUL, *J. Mater. Sci.* **16** (1981) 1769.
3. C. P. CHEN and M. H. LEIPOLD, *Amer. Ceram. Soc. Bull.* **59** (1980) 469.
4. V. G. EREMENKO and V. I. NIKITENKO, *Phys. Status Solidi (a)* **14** (1972) 317.
5. J. R. PATEL, *J. Appl. Phys.* **34** (1963) 2788.
6. S. DANYLUK and R. REAVES, *Wear* **77** (1982) 81.
7. K. V. RAVI, *"Imperfections and Impurities in Semiconductor Silicon"* (Wiley, New York, 1981) p. 17.
8. C. P. MARDEN, (editor), "Silicon Device Processing" (NBS Special Publications No. 337, US Department of Commerce, Washington, D.C., 1970) p. 419.
9. C. P. CHEN, *J. Electrochem. Soc.* **129** (1982) 2835.
10. S. W. LEE, D. S. LIM and S. DANYLUK, *J. Mater. Sci. Lett.* **3** (1984) 651.
11. J. J. MECHOLSKY, R. W. RICE and S. W. FRIEMAN, *J. Amer. Ceram. Soc.* **57** (1974) 440.
12. G. K. BANSAL, *Phil. Mag.* **35** (1977) 935.
13. J. J. MECHOLSKY and M. G. DREXHAGE, *J. Amer. Ceram. Soc.* **63** (1980) 347.
14. S. W. FREIMAN, A. C. GONZALEZ and J. J. MECHOLSKY, *ibid.* **62** (1979) 206.
15. R. M. GRUVER and H. P. KIRCHNER, *ibid.* **57** (1974) 220.
16. W. C. DASH, *J. Appl. Phys.* **27** (1956) 1193.

Received 30 November
and accepted 19 December 1984